

## Electron capture by doubly charged ions from laser-excited alkali atoms: II. $\text{He}^{2+}$ – $\text{Li}^*(2p)$ collisions

M Gieler†, F Aumayr†, M Weber†, H P Winter† and J Schweinzer‡

† Institut für Allgemeine Physik, Technische Universität Wien, Wiedner Hauptstrasse 8–10, A-1040 Wien, Austria

‡ Max Planck Institut für Plasmaphysik, D-8046 Garching, Federal Republic of Germany

Received 30 December 1992, in final form 8 April 1993

**Abstract.** Single electron capture in collisions of slow ( $\text{keV amu}^{-1}$ )  $\text{He}^{2+}$  ions with aligned  $\text{Li}^*(2p)$  atoms has been investigated by means of translational energy spectroscopy. A single mode cw dye laser beam has been modified by using an electro-optical modulator in order to pump both hyperfine ground states of Li simultaneously, thus maximizing the fraction of excited target atoms.

Cross sections for electron capture from  $\text{Li}(2s)$ ,  $\text{Li}^*(2p\Sigma)$  and  $\text{Li}^*(2p\Pi)$  initial states into  $\text{He}^+(n = 3, 4, 5)$  final states have been determined for different impact energies and compared with 68-state atomic orbital (AO) close coupling calculations.

### 1. Introduction

In contrast to collisions of doubly charged ions with ground state alkali atoms which have been studied systematically for some time (e.g. Schweinzer and Winter 1990a, b and references cited therein), experimental and theoretical investigations involving laser-excited alkali target states have started only recently (Aumayr *et al* 1992a, Gieler *et al* 1993a). This paper is the second in a series of combined experimental and theoretical studies on single electron capture (SEC) in collisions of doubly charged ions with laser-excited alkali atoms. Whereas detailed results for the  $\text{He}^{2+}$ – $\text{Na}^*(3p)$  collision system have been presented in the first paper (Gieler *et al* 1993b, hereafter referred to as I), the present paper presents the first experimental and advanced theoretical study (sections 2–4) on SEC in collisions of  $\text{He}^{2+} + \text{Li}^*(2p)$ .

Investigations of collision processes involving excited  $\text{Li}^*(2p)$  atoms are not only of fundamental interest, but also important for diagnostics of magnetically confined fusion plasmas by means of Li beam spectroscopy (Aumayr and Winter 1985). Injection of a beam of fast ( $1\text{--}10 \text{ keV amu}^{-1}$ ) neutral lithium atoms into a tokamak plasma has been shown to provide a wide range of diagnostic possibilities. By analysing line radiation following collisions of Li atoms with plasma particles, important parameters of the plasma edge such as electron density (McCormick and the ASDEX team 1985, Schweinzer *et al* 1992b, Aumayr *et al* 1992b), local electric and magnetic field (Rebhan *et al* 1981, Fujita and McCormick 1973) strengths as well as densities (Schorn *et al* 1991) and temperatures (Schorn *et al* 1992) of impurity ions can be determined.

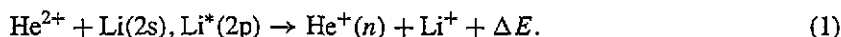
Measuring electron densities (Li-IXS, impact lithium excitation spectroscopy) is based on the detection of the  $\text{Li}(2s\text{--}2p)$  resonance line at 670.8 nm, which becomes excited by collisions with the plasma particles. SEC from Li into highly excited states of impurity

ions is followed by their characteristic line radiation, in particular in the visible region, which provides a detection method (lithium charge exchange spectroscopy/Li-CXS) for these plasma impurities with improved signal-to-noise ratio in comparison to standard hydrogen diagnostic beams (Winter 1982).

However, the success of these methods is strongly connected to the availability of reliable data on reaction cross sections for collisions of the plasma particles such as electrons, protons and multiply charged impurity ions, not only with ground state Li(2s) but also with excited Li\*(2p) (cf section 5).

## 2. Experiment

The investigations were carried out by using the same experimental set-up as described in detail in I. It consisted of a translational energy (TE) spectrometer for studying state-selective electron capture in collisions of He<sup>2+</sup> with ground state as well as laser-excited Li atoms:



In a crossed beam geometry the mass selected ion beam, a highly collimated lithium atom beam and a resonant dye laser beam (670.78 nm) intersected each other under 90°.

Usually, preparation of <sup>7</sup>Li and <sup>23</sup>Na atoms (which have similar level schemes) is performed by using single mode CW dye laser radiation tuned to the D<sub>2</sub> <sup>2</sup>S<sub>1/2</sub> F<sub>1</sub> = 2 → <sup>2</sup>P<sub>3/2</sub> F<sub>u</sub> = 3 transition (cf Fischer and Hertel 1982, Gieler *et al* 1993a, and the corresponding hyperfine level scheme of Li in figure 1). Whereas Na is isotopically pure in its natural occurrence, Li contains 7.5% <sup>6</sup>Li, which due to its isotope shift cannot be excited simultaneously with <sup>7</sup>Li under our experimental conditions. Assuming ideal stationary optical pumping conditions (two-level atom and sufficient pumping power to saturate this transition) and considering the statistical weight ( $\frac{5}{8}$ ) of the <sup>2</sup>S<sub>1/2</sub> F<sub>1</sub> = 2 hyperfine ground state, a maximum fraction  $f^* = ((\frac{1}{2}) \times (\frac{5}{8})) = 31.25\%$  of the <sup>7</sup>Li atoms can be excited.

However, a number of factors may disturb the optical pumping process. Various line broadening effects (e.g. power broadening, Doppler broadening, etc...) give rise to an overlap of the F<sub>u</sub> = 3 and F<sub>u</sub> = 2 hyperfine levels of <sup>2</sup>P<sub>3/2</sub>, such that in the cycles of excitation and de-excitation the atoms can also decay to the <sup>2</sup>S<sub>1/2</sub> F<sub>1</sub> = 1 ground state by spontaneous emission. Since the latter is not in resonance with the laser field, the corresponding atoms become trapped in the ground state (HFS trapping). In fact, Gieler *et al* (1993a) have shown that HFS trapping limits the fraction of excited atoms in the case of Na to typically 10%. As a consequence, an electro-optical modulator (EOM) has been applied as described by Gieler *et al* (1993a), to pump both F<sub>1</sub> = 2 → F<sub>u</sub> = 3 and F<sub>1</sub> = 1 → F<sub>u</sub> = 2 transitions by using first-order side-bands. In this way an excitation efficiency of typically 30% could be achieved.

When pumping Li, the effect of HFS trapping is more pronounced than for Na, since the <sup>2</sup>P<sub>3/2</sub> F<sub>u</sub> = 0, 1, 2, 3 states are situated within only 18.1 MHz (cf figure 1), compared to 60 MHz in the case of Na. Indeed, first TE spectra from He<sup>2+</sup>-Li collisions showed a fraction of excited Li atoms in the target beam of a few per cent only, if single-mode excitation was used. In the case of Li the use of an EOM was therefore mandatory to provide a sufficiently large excitation efficiency.

The resonator of the available EOM was optimized to match the F<sub>1</sub> = 2 → F<sub>u</sub> = 3 and F<sub>1</sub> = 1 → F<sub>u</sub> = 2 for Na by the two first-order side-bands with a corresponding microwave frequency of 856 MHz (Gieler *et al* 1993a).

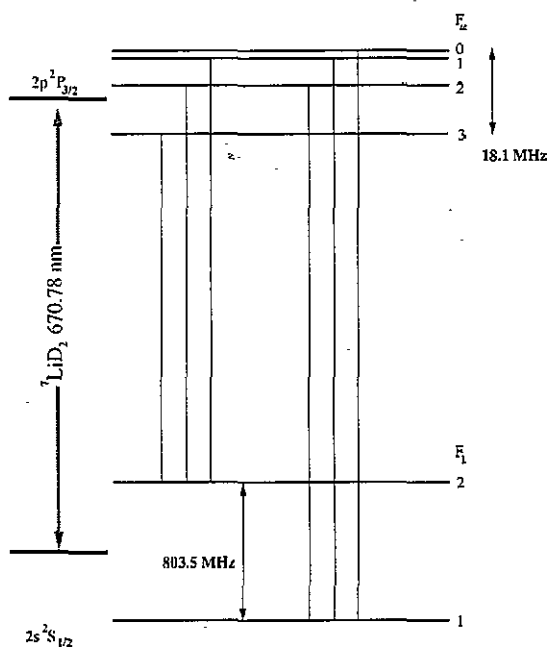


Figure 1. Energy levels related to the  $D_2$  line of  $^7\text{Li}$  (not to scale) and possible dipole transitions.

The same device can in principle also be applied to pump the  $^7\text{Li } 2S_{1/2} F_1 = 2 \rightarrow 2P_{3/2} F_u = 3$  and  $F_1 = 1 \rightarrow F_u = 2$  transitions, by using the zero-order and one of the two first-order side-bands of the modulated laser light separated by approximately 850 MHz. Since the hyperfine splitting of the ground state of Li is about 803.5 MHz (cf figure 1), a perfect frequency match could not be obtained, because the  $Q$  value of the EOM resonator decreased strongly for microwave frequencies far below 850 MHz.

Nevertheless, sufficient pumping efficiency could be achieved as a combined result of power and Doppler broadening affecting the excited Li beam.

Figure 2 shows typical TE spectra (energy resolution  $\approx 0.4$  eV FWHM) for 1 keV  $\text{amu}^{-1}$   $\text{He}^{2+}$  impact on Li obtained for the cases of 'laser off' and two mode excitation 'laser on', respectively (linear laser light polarization perpendicular to the ion beam direction).

Electron capture from ground state Li(2s) primarily populates  $\text{He}^+(n = 3)$  states, but capture into ( $n = 4$ ) can also be identified. In the TE spectrum recorded with 'laser on' the projectiles interacted with a mixed target of ground state Li(2s) (fraction  $1 - f^*$ ) and excited state  $\text{Li}^*(2p)$  atoms (fraction  $f^*$ ). Additional peaks in the 'laser on' TES have to be attributed to capture from  $\text{Li}^*(2p)$  because of their exothermic energy shift of 1.85 eV with respect to the corresponding peak positions in the 'laser off' spectrum. As discussed in I, the fraction of excited atoms in the target beam can be determined from the decrease of the peak at  $\Delta E = +0.66$  eV (corresponding to capture from ground state Li(2s) into  $\text{He}^+(n = 3)$ ).

As demonstrated by figure 2, a pumping efficiency of typically  $f^* = 20\%$  could be achieved, despite the frequency mismatch discussed above.

In addition, the influence of the EOM on the resulting state of target polarization, i.e. relative magnetic sublevel population, a quantity relevant for studying alignment effects in collision experiments has been investigated by polarization measurements (cf I). As already outlined by Gieler *et al* (1993a), only a slight loss of polarization quantity for two-mode

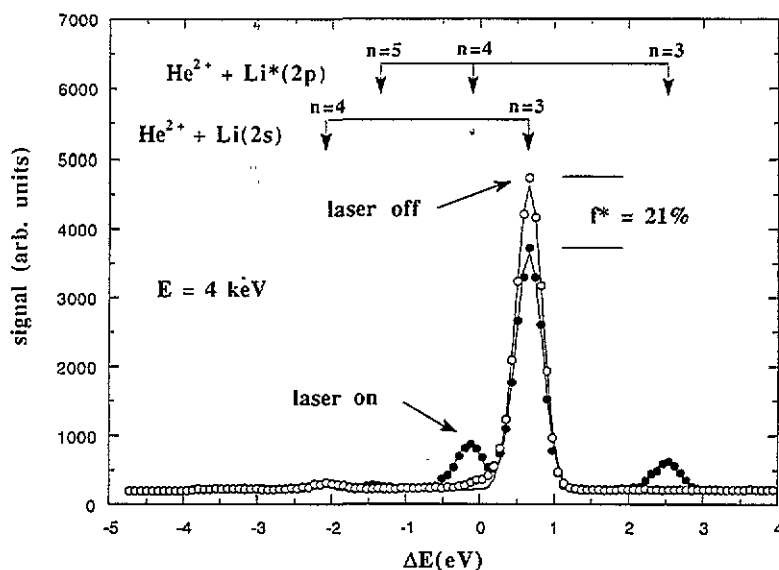


Figure 2. Translational energy spectra for impact of  $1 \text{ keV amu}^{-1} {}^4\text{He}^{2+}$  on Li. Comparison is made between spectra measured with 'laser on' (full symbols) and 'laser off' (open symbols) respectively. The different final  $\text{He}^+(n)$  states for capture from respectively Li(2s) and Li\*(2p) have been indicated by arrows. Compared to 'laser off', in the 'laser on' TE spectrum additional peaks occur, whereas the attenuation of the main peak corresponds with the transfer of a target atom fraction  $f^*$  into the excited Li\*(2p) state.

excitation as compared to single-mode pumping has been found and has been taken into account.

### 3. AO calculations

The well known semiclassical approach of expanding the total electron scattering wavefunction into target and projectile centred travelling atomic orbitals (AO), and solving the time-dependent Schrödinger equation in this truncated Hilbert space has been applied (Nielsen *et al* 1990). The projectile centred part of the basis consists of the complete  $n = 1, 2, 3, 4, 5$  shells (cf I). These states are taken as exact  $Z = 2$  hydrogen-like states. The radial wavefunctions for the Li( $n = 2, 3$ ) states are approximated by effective charge hydrogenic states with  $Z$  values of 1.26, 1.155, 1.02, 1.015, and 1.0005 for Li(2s), Li\*(3s), Li\*(2p), Li\*(3p) and Li\*(3d), respectively. This set of wavefunctions consists of eigenstates of different Hamiltonians and is therefore not fully orthogonal. The small overlaps between states with the same angular momentum but different  $n$  quantum number have been neglected in the close coupling calculations. However, the initial charge cloud distribution in collisions of  $\text{He}^{2+}$  with aligned Li\*(2p) atoms should be described with sufficient accuracy, considering the almost hydrogenic effective charge value (see above) of the Li\*(2p) state.

Couplings between projectile states induced by the electric field of the Li<sup>+</sup> core are calculated by assuming a pure Coulomb interaction potential.

The convergence of our calculations could not be tested by further inclusion of the complete ( $n = 6$ ) principal shell on the projectile centre which would involve large scale

computations. However, numerical results have been found to be insensitive to additional inclusion of  $6s, p$  states to the above described basis set (AO68). For more details on the calculation procedure see I. Results of the present AO68 calculations have been listed in table 1.

Table 1. Calculated cross sections (in units of  $10^{-16} \text{ cm}^2$ ) for SEC into  $\text{He}^+(n = 3, 4, 5)$  final states in collisions of  $\text{He}^{2+}$  with  $\text{Li}^*(2p\Sigma)$ ,  $\text{Li}^*(2p\Pi^+)$  and  $\text{Li}^*(2p\Pi^-)$ , respectively, plotted against ion impact energy.

(a) initial state  $\text{Li}^*(2p\Sigma)$

$E \text{ (keV amu}^{-1}\text{)}$	$\sigma_{\Sigma}(3)$	$\sigma_{\Sigma}(4)$	$\sigma_{\Sigma}(5)$
1.0	62	55	15
1.5	67	55	14
2.0	68	46	18
2.5	64	35	22
4.0	56	33	25
8.0	33	23	14
16.0	11	11	9

(b) initial state  $\text{Li}^*(2p\Pi^+)$

$E \text{ (keV amu}^{-1}\text{)}$	$\sigma_{\Pi^+}(3)$	$\sigma_{\Pi^+}(4)$	$\sigma_{\Pi^+}(5)$
1.0	36	150	11
1.5	27	189	17
2.0	25	190	20
2.5	26	173	20
4.0	27	114	31
8.0	16	33	24
16.0	6	5	4

(c) initial state  $\text{Li}^*(2p\Pi^-)$

$E \text{ (keV amu}^{-1}\text{)}$	$\sigma_{\Pi^-}(3)$	$\sigma_{\Pi^-}(4)$	$\sigma_{\Pi^-}(5)$
1.0	63	15	1
1.5	65	27	1
2.0	65	37	3
2.5	62	40	4
4.0	58	41	4
8.0	31	24	8
16.0	6	7	5

#### 4. Results and discussion

'Pure'  $\text{Li}^*(2p_{\perp})$ - and  $\text{Li}^*(2p_{\parallel})$ -related translational energy spectra/TES (cf below) could be obtained by properly subtracting and scaling TES for 'laser on' and 'laser off' as described in I. Results for  $1 \text{ keV amu}^{-1}$  impact energy are presented in figures 3(a)–(c). Figure 3(a) shows a TES for collisions with ground state  $\text{Li}(2s)$  atoms and illustrates the dominance of capture into the  $\text{He}^+(n = 3)$  state. Figures 3(b) and (c) display TES for capture from excited  $\text{Li}^*(2p)$  atoms with laser light polarization in parallel (b) and perpendicular (c) to the ion beam direction, respectively.

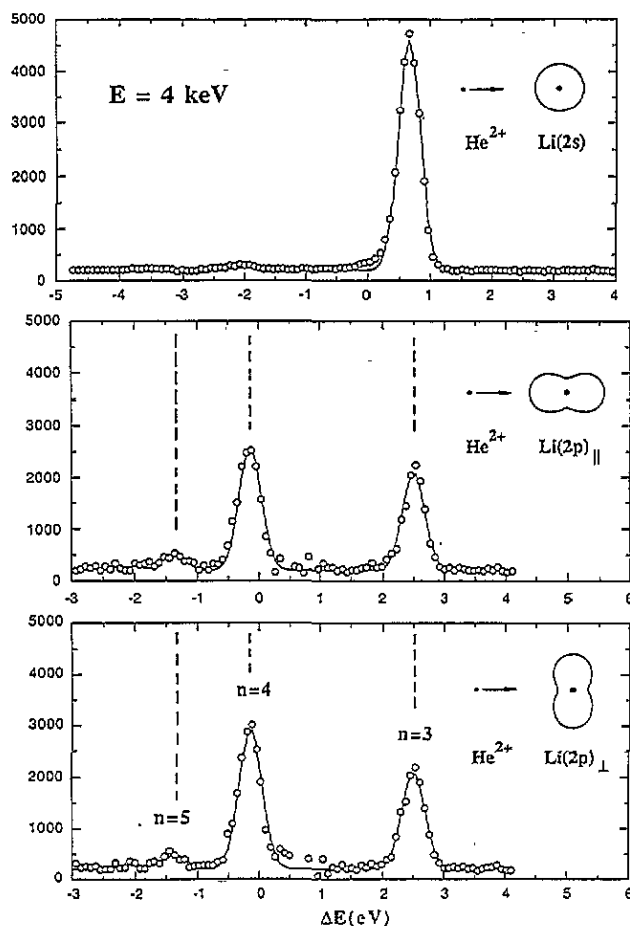


Figure 3. Translational energy spectra for impact of  $1 \text{ keV amu}^{-1} {}^4\text{He}^{2+}$  on (a)  $\text{Li}(2s)$  (upper panel), (b)  $\text{Li}^*(2p)$  with laser light polarization parallel (middle panel) and, (c) perpendicular (lower panel) to the  $\text{He}^{2+}$  beam direction. plotted against the reaction energy defect  $\Delta E$ . The different final  $\text{He}^+(n)$  states for capture from respectively  $\text{Li}(2s)$  and  $\text{Li}^*(2p)$  have been indicated by vertical broken lines. In addition, the shape of the  $\text{Li}$  valence electron charge cloud prior to the collision is illustrated, with laser light incident perpendicular to the figure plane.

From figure 3 it is obvious that the state selectivity of the electron capture process is changed for capture from excited  $\text{Li}^*(2p)$  in comparison to capture from ground state  $\text{Li}(2s)$  atoms, as similarly observed for  $\text{He}^{2+}\text{-Na}$  collisions (I).

At  $1 \text{ keV amu}^{-1}$  impact energy, capture into  $\text{He}^+(n=4)$  and  $\text{He}^+(n=5)$  states is strongly enhanced with  $\text{Li}^*(2p)$ . On the other hand, capture into  $\text{He}^+(n=3)$  decreases significantly.

Furthermore, comparison of figures 3(b) and 3(c) reveals that the probability for capture into  $\text{He}^+(n=4)$  decreases if the laser polarization is rotated from perpendicular to parallel to the ion beam direction.

From these TES, relative cross sections  $\sigma_{2p\Sigma}(n)/\sigma_{2s}(n=3)$  and  $\sigma_{2p\Pi}(n)/\sigma_{2s}(n=3)$  for electron capture from  $\text{Li}^*(2p)$  into the  $\text{He}^+(n=3, 4, 5)$  final states in comparison to capture from  $\text{Li}(2s)$  into the dominant  $\text{He}^+(n=3)$  state have been determined (for definition of  $\Sigma$  and  $\Pi$  states of I).

In order to obtain absolute experimental cross sections for SEC from  $\text{Li}^*(2p)$ , a normalization to data for  $\text{He}^{2+} + \text{Li}(2s)$  has been performed. In figure 4 experimental and theoretical total cross sections for  $\text{He}^{2+} + \text{Li}(2s)$  collisions available from the literature are plotted together with the results of the present AO68 calculations. The theoretical data reported by Fritsch and Lin (1983) perfectly agree with most of the experimental results and are therefore used for normalization. The results of our calculations overestimate the cross sections at impact energies  $E > 2 \text{ keV amu}^{-1}$ . This deviation is probably caused by our choice of the  $\text{Li}(2s)$  wavefunction (see section 3). Since we are interested mainly in capture from the  $\text{Li}^*(2p)$  states, we have not further optimized our calculations for capture from  $\text{Li}(2s)$  ground state.

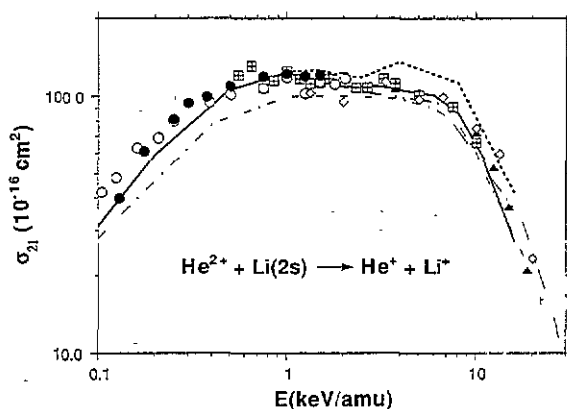


**Figure 4.** Experimental and calculated cross sections for total sec in  $\text{He}^{2+}$ - $\text{Li}(2s)$  collisions plotted against impact energy. Experimental results:  $\boxplus$ , Dijkamp *et al* (1985);  $\diamond$ , DuBois and Toburen (1985);  $\blacktriangle$ , Kadota *et al* (1982);  $\bullet$ , Schweinzer and Winter (1990a);  $+$ , Shah *et al* (1985);  $\odot$ , Varghese *et al* (1984). Calculated results:  $\cdots$ , this work;  $- \cdot -$ , Ermolaev and Hewitt (1985);  $---$ , Fritsch and Lin (1983);  $- \cdot \cdot -$ , Sato and Kimura (1983).

Partial cross sections for capture into  $\text{He}^+(n = 3, 4, 5)$  states from  $\text{Li}(2s)$  are given in figure 5. The results of the calculations of Fritsch and Lin (1983) and our calculations are compared with the experimental data of Aumayr *et al* (1989) and our experimental results from the 'laser off' TE spectra. Generally both sets of theoretical data reproduce the experimental results quite well. Our  $\text{He}^+(n = 4, 5)$  data are somewhat smaller than the ones from Aumayr *et al* (1989) which might reflect scattering losses of the  $\text{He}^+$  projectiles. For these measurements our translational energy spectrometer has an angular acceptance of only  $\pm 0.15^\circ$  (cf discussion in I).

In figures 6(a) and 6(b) absolute experimental cross sections for capture into  $\text{He}^+(n = 3, 4, 5)$  from  $\text{Li}^* 2p\Pi$  and  $2p\Sigma$  initial states are compared with the theoretical results of the AO68 calculation. Table 2 gives the corresponding experimental partial cross sections.

Experimental and theoretical data are in excellent agreement for SEC from  $2p\Pi$  into  $\text{He}^+(n = 3, 4, 5)$ , whereas only fair agreement exists in the case of the  $2p\Sigma$  initial state, since the theoretical cross sections are considerably larger than the experimental ones. The same behaviour has already been observed for the corresponding  $\text{He}^{2+} + \text{Na}^*(3p\Sigma, 3p\Pi)$  collision systems (cf discussion in I). From a theoretical viewpoint it is difficult to give an explanation for this disagreement, but we suppose that intermediate population of  $(n = 6)$  states with high angular momentum might influence the capture process considerably.

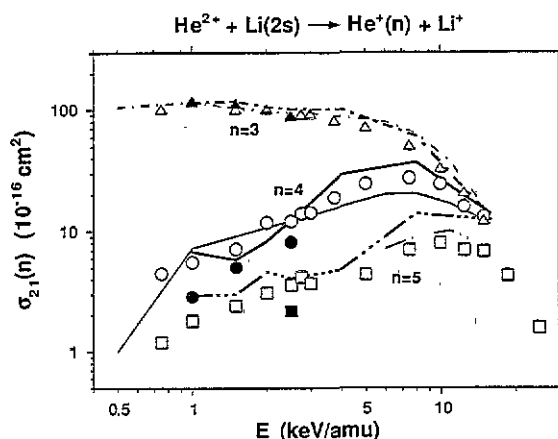


Figure 5. Experimental and calculated cross sections for SEC in  $\text{He}^{2+}$ -Li(2s) collisions into  $\text{He}^+(n = 3, 4, 5)$  final states, plotted against impact energy. Comparison is made between experimental results of this work and Aumayr *et al* (1989), as well as calculated results of this work (thick lines) and Fritsch and Lin (1983) (thin lines).

Experimental results		
SEC into	This work	Aumayr <i>et al</i> (1989)
$\text{He}^+(n = 3)$	▲	△
$\text{He}^+(n = 4)$	●	○
$\text{He}^+(n = 5)$	■	□
Calculated results		
SEC into	This work	Fritsch and Lin (1983)
$\text{He}^+(n = 3)$	— · — · —	— · —
$\text{He}^+(n = 4)$	— — —	— — —
$\text{He}^+(n = 5)$	— · · · —	— · · · —

At low impact energies mainly  $\text{He}^+(n = 4)$  and  $\text{He}^+(n = 3)$  contribute to the total cross sections, whereas  $\text{He}^+(n = 5)$  cross sections are comparably small.

This selectivity is somewhat washed out at higher impact energies, where all partial cross sections are of comparable magnitude both for the  $\Pi$  and in the  $\Sigma$  systems.

The agreement of experimental and theoretical alignment parameters  $A(n)$  (cf figure 7) is not fully satisfactory, though considerably large experimental errors preventing a critical judgment of our theoretical approach. However, much of these deviations are probably due to the discrepancies in the  $\Sigma$  cross sections. As in the  $\text{He}^{2+} + \text{Na}^*(3p\Sigma, 3p\Pi)$  case, the experimental  $A(4)$  values are negative, whereas  $A(3)$  and  $A(5)$  tend to be slightly positive.

However, our calculations show that with increasing impact energy the alignment parameters  $A(n)$  (cf I) approach each other and eventually achieve positive values (cf figure 7), a trend that has also been observed for Na (cf I and Schlattmann *et al* (1993)).

## 5. Implications for Li beam edge plasma spectroscopy

Determination of electron and impurity density profiles by means of Li-IXS and Li-CXS (see section 1) requires modelling of the attenuation and composition of the neutral lithium beam on its way into the plasma. For this modelling procedure, the knowledge of atomic data



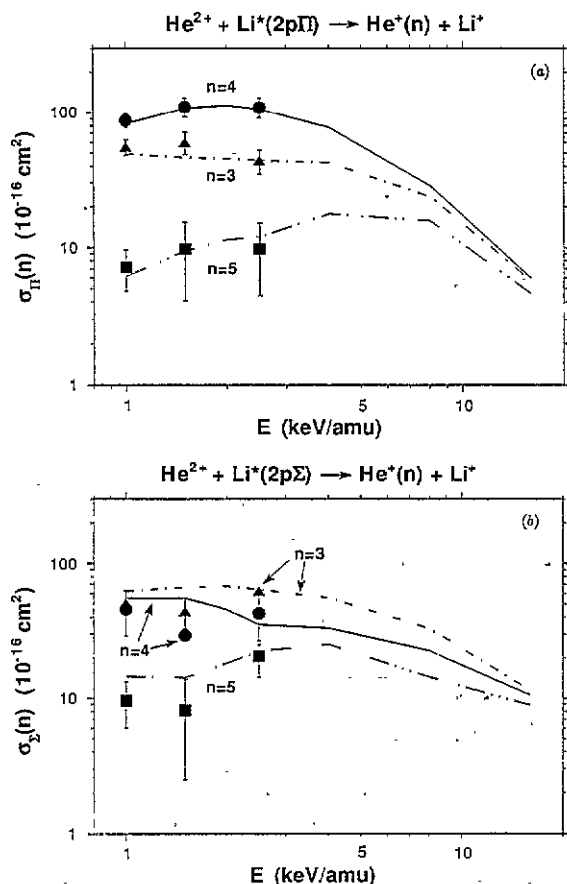


Figure 6. Experimental and calculated cross sections for SEC into  $\text{He}^+(n = 3, 4, 5)$  final states in collisions of  $^4\text{He}^{2+}$  with (a)  $\text{Li}^*(2p\Pi)$ , (b)  $\text{Li}^*(2p\Sigma)$  plotted against ion impact energy. Comparison is made between present experimental data (symbols) and results of our AO68 calculations (thick lines).

	Experimental results	Calculated results
$\text{He}^+(n = 3)$	▲	— · —
$\text{He}^+(n = 4)$	●	—
$\text{He}^+(n = 5)$	■	— · · —

for various collision processes of neutral Li atoms in ground as well as excited states with protons, electrons and impurity ions is essential for accurate evaluation of both Li-IXS and Li-CXS data. An atomic data base covering collisions of  $\text{Li}(nl, n \leq 3)$  with electrons and protons has recently been collected by Aumayr *et al* (1993).

Present evaluation procedures for reconstruction of electron density profiles from Li-IXS emission profiles suffer from the lack of sufficiently accurate atomic data for collisions of multicharged impurity ions with  $\text{Li}(nl)$  atoms (Schweitzer *et al* 1992a). Although the fraction of  $\text{Li}^*(2p)$  in the injected beam may reach a maximum value of 15% only (cf Schweitzer *et al* 1992a), charge exchange of these excited Li atoms with impurity ions is quite important for the attenuation of the neutral Li beam, because of the enhanced total SEC cross section in comparison to  $\text{Li}(2s)$ . From the viewpoint of lithium beam plasma

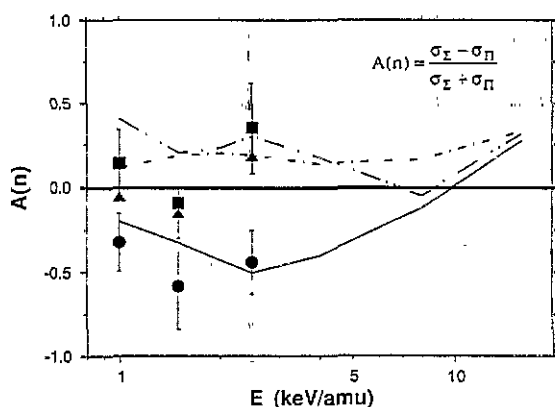


Figure 7. The  $\Sigma$ - $\Pi$  alignment parameter  $A(n)$  for  $\text{He}^+(n = 3, 4, 5)$  final states plotted against incident  $^4\text{He}^{2+}$  energy. Experimental data (symbols) are compared with the results of AO68 calculations.

	Experimental results	Calculated results
$A(3)$	▲	— · —
$A(4)$	●	—
$A(5)$	■	— · · —

Table 2. Experimental cross sections (in units of  $10^{-16} \text{ cm}^2$ ) for SEC into  $\text{He}^+(n = 3, 4, 5)$  final states in collisions of  $\text{He}^{2+}$  with  $\text{Li}^*(2p\Sigma)$ ,  $\text{Li}^*(2p\Pi)$ , respectively, plotted against ion impact energy. Error bars neither include normalization of our results to data for  $\text{He}^{2+}$ - $\text{Li}(2s)$  collisions nor limited acceptance. The alignment parameters  $A(n = 3, 4, 5)$  are also tabulated.

$E \text{ (keV amu}^{-1}\text{)}$	$\sigma_\Sigma(3)$	$\sigma_\Pi(3)$	$\sigma_\Sigma(4)$	$\sigma_\Pi(4)$	$\sigma_\Sigma(5)$	$\sigma_\Pi(5)$
1.0	$50 \pm 12$	$55 \pm 7$	$46 \pm 17$	$88 \pm 11$	$10 \pm 4$	$7 \pm 3$
1.5	$44 \pm 11$	$60 \pm 11$	$29 \pm 26$	$110 \pm 18$	$8 \pm 6$	$10 \pm 6$
2.5	$62 \pm 13$	$44 \pm 9$	$14 \pm 18$	$109 \pm 18$	$20 \pm 6$	$10 \pm 5$
$E \text{ (keV amu}^{-1}\text{)}$	$A(3)$	$A(4)$	$A(5)$			
1.0	$-0.05 \pm 0.13$	$-0.32 \pm 0.17$	$0.14 \pm 0.20$			
1.5	$-0.15 \pm 0.15$	$-0.58 \pm 0.26$	$-0.1 \pm 0.60$			
2.5	$0.18 \pm 0.14$	$-0.44 \pm 0.19$	$0.35 \pm 0.27$			

spectroscopy, both collision systems  $\text{He}^{2+}$ - $\text{Li}(2s, 2p)$ ,  $\text{Na}(3s, 3p)$  have been considered as a testing ground for the close coupling approach to be used in future calculations for producing required cross sections not only for SEC but also for excitation of the injected Li atoms in collisions with impurity ions ( $\text{Be}^{q+}$ ,  $\text{B}^{q+}$ ,  $\text{C}^{q+}$ ).

As already explained in the introduction, for utilization of Li-CXS in fusion edge plasmas there is a need for  $n, l$  selective cross sections for SEC by the impurity ions of interest from both  $\text{Li}(2s)$  and  $\text{Li}^*(2p)$ . Beyond the respectively dominantly populated final principal shell the SEC cross sections decrease again, whereas the wavelengths for  $n \rightarrow n - 1$  optical transitions increase with further increasing  $n$ . However, the considerably more convenient detection in the visible as compared to the VUV region may outweigh the decreasing emission cross sections for higher  $n$ . A non-negligible  $\text{Li}^*(2p)$  fraction in the active Li beam will principally enhance the cross sections for SEC into the higher  $n$  shells, as can be demonstrated

for  $\text{He}^{2+}$  (i.e. He ash detection in the plasma edge).  $\text{He}^{2+}$  ions can be conveniently detected via the  $\text{He II}(n = 4 \rightarrow n = 3)$  transitions at 468.8 nm (Aumayr *et al* 1989). In figure 8, we have sketched the relative populations of the  $\text{He}^+(n = 3)$  and  $\text{He}^+(n = 4)$  shells as resulting from impact of  $2.5 \text{ keV amu}^{-1}$   $\text{He}^{2+}$  on respectively  $\text{Li}(2s)$  and  $\text{Li}^*(2p)$ , a situation corresponding to the injection of a  $17.5 \text{ keV } ^7\text{Li}$  beam into the edge plasma. Assuming only 15%  $\text{Li}^*(2p)$  fraction in the beam, the latter would already contribute with 50% to the total  $\text{He}^+(n = 4)$  population.

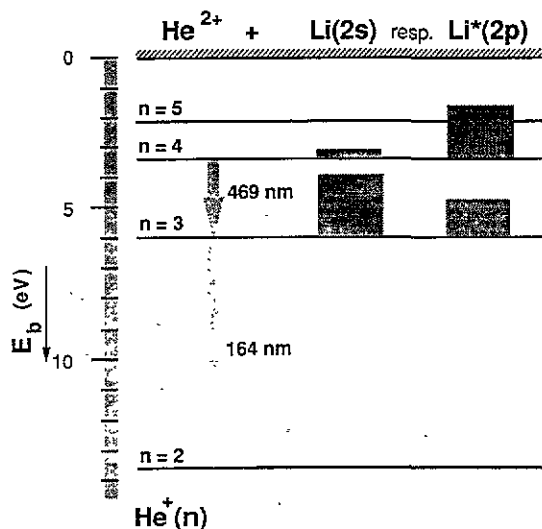


Figure 8. Relevant  $\text{He}^+$  final states for electron capture in  $2.5 \text{ keV amu}^{-1}$   $\text{He}^{2+}\text{-Li}$  collisions, with He II binding energies ( $E_b$ ) and energy scale. Bars indicate relative capture probabilities into  $\text{He}^+(n = 3, 4)$  final states for collisions with  $\text{Li}(2s)$  and  $\text{Li}^*(2p)$  initial states, respectively.

## 6. Conclusions

Absolute experimental cross sections for electron capture from  $\text{Li}^*(2p\Sigma)$  and  $\text{Li}^*(2p\Pi)$  initial states into  $\text{He}^+(n = 3, 4, 5)$  final states have been determined at different  $\text{He}^{2+}$  impact energies. The data can be satisfactorily reproduced by AO68 calculations covering the most relevant reaction channels.

The results are of considerable importance for diagnostics of magnetically confined fusion plasmas by means of Li beam spectroscopy, because excited  $\text{Li}^*(2p)$  atoms essentially contribute to the  $\text{Li}^0$  beam attenuation and emission of characteristic line radiation caused by capture reactions. The  $\text{He}^{2+}\text{-Li}$  collision system investigated provides a model case for further suggested experimental and theoretical work on interaction of plasma particles with  $\text{Li}^*(2p)$  excited atoms.

## Acknowledgments

This work has been supported by Austria Fonds zur Förderung der wissenschaftlichen Forschung (project no P7006PHY) and by Kommission zur Koordination der Kernfusionsforschung at the Austrian Academy of Sciences. We thank Dr W Husinsky for providing

the dye laser system for these experiments. Participation of P Ullmann during the measurements is also acknowledged. We thank Mr J P Hansen for providing the computer code used.

## References

- Aumayr F, Gieler M, Schweinzer J, Winter H P and Hansen J P 1992a *Phys. Rev. Lett.* **68** 3277
- Aumayr F, Janev R K, Schneider M, Smith J J, Wutte D, Schweinzer J and Winter H P 1993 *Report IAEA-INDC-NDS 267 IAEA* in print
- Aumayr F, Schorn R P, Pöckl M, Schweinzer J, Wolfrum E, McCormick K, Hintz E and Winter H P 1992b *J. Nucl. Mat.* **196-198** 928
- Aumayr F, Schweinzer J and Winter H P 1989 *J. Phys. B: At. Mol. Opt. Phys.* **22** 1027
- Aumayr F and Winter H P 1985 *Ann. Phys., Lpz.* **42** 228
- Dijkamp D, Boellard A and deHeer F J 1985 *Nucl. Instrum. Methods B* **9** 377
- DuBois F D and Toburen L H 1985 *Phys. Rev. A* **31** 3603
- Ermolaev A M and Hewitt R N 1985 *Nucl. Instrum. Methods B* **9** 377
- Fischer A and Hertel I V 1982 *Z. Phys. A* **304** 103
- Fritsch W and Lin C D 1983 *J. Phys. B: At. Mol. Phys.* **16** 1595
- Fujita J and McCormick K 1973 *Proc. 6th Eur. Conf. on Controlled Fusion and Plasma Physics (Moscow)* p 191
- Gieler M, Aumayr F, Gaggi R, Neureiter C and Windholz L 1993a *J. Phys. B: At. Mol. Opt. Phys.* **26** 297
- Gieler M, Aumayr F, Schweinzer J, Koppensteiner W, Husinsky W, Winter H P, Lozhkin K and Hansen J P 1993b *J. Phys. B: At. Mol. Opt. Phys.* **26** 2137-51
- Gieler M, Aumayr F and Windholz L 1992 *Phys. Rev. Lett.* **69** 3452
- Kadota K, Dijkamp D, van der Woude R L, Yan P G and deHeer F J 1982 *J. Phys. B: At. Mol. Phys.* **15** 3297
- McCormick K and the ASDEX team 1985 *Rev. Sci. Instrum.* **56** 1063
- Nielsen S E, Hansen J P and Dubois A 1990 *J. Phys. B: At. Mol. Opt. Phys.* **23** 2595
- Rebhan U, Wiegart N J and Kunze H-J 1981 *Phys. Lett.* **85A** 228
- Sato H and Kimura M 1983 *Phys. Lett.* **96A** 286
- Schlatmann A R, Hoekstra R, Mook H W and Morgenstern R 1993 *Highly Charged Ions (Phys. Conf. Proc.)* (New York: AIP) at press
- Schorn R P, Hintz E, Rusbüldt D, Aumayr F, Schneider M, Unterreiter E and Winter H P 1991 *Appl. Phys. B* **52** 71
- Schorn R P, Wolfrum E, Aumayr F, Hintz E, Rusbüldt D and Winter H P 1992 *Nucl. Fusion* **32** 351
- Schweinzer J, McCormick K, Fiedler S, Aumayr F, Pöckl M and Winter H P 1992a *Proc. 19th EPS Conf. on Controlled Fusion and Plasma Physics (Innsbruck)* Abstracts 16C II-1163
- Schweinzer J and Winter H P 1990a *J. Phys. B: At. Mol. Opt. Phys.* **23** 3881
- 1990b *J. Phys. B: At. Mol. Opt. Phys.* **23** 3899
- Schweinzer J, Wolfrum E, Aumayr F, Pöckl M, Winter H P, Schorn R P, Hintz E and Unterreiter A 1992b *Plasma Phys. Contr. Fusion* **34** 1173
- Shah M B, Elliot D S and Gilbody H B 1985 *J. Phys. B: At. Mol. Phys.* **18** 4245
- Varghese S L, Waggoner W and Cocke C L 1984 *Phys. Rev. A* **29** 2453
- Winter H P 1982 *Comment. At. Mol. Phys.* **12** 165